ELSEVIER

International Journal of Mass Spectrometry 194 (2000) 53–68

International Journal of Mass Spectrometry

Laboratory investigations of negative ion molecule reactions of propionic, butyric, glyoxylic, pyruvic, and pinonic acids

Jyrki Viidanoja[1,*], Thomas Reiner[2], Astrid Kiendler, Frank Grimm, Frank Arnold

Atmospheric Physics Division, Max-Planck-Institute for Nuclear Physics, P. O. Box 103980, D-69029 Heidelberg, Germany

Received 23 June 1999; accepted 9 August 1999

Abstract

We have carried out laboratory measurements of gas-phase ion-molecule-reactions of several negative ion species with propionic, butyric, glyoxylic, pyruvic, and pinonic acids. A flow reactor operating at a temperature of 293 ± 3 K and total gas pressures of 1.5 hPa, 9 hPa, or 40 hPa were used. The negative reagent ion species investigated included CO_3^-, $CO_3^-H_2O$, NO_3^-, $NO_3^-H_2O$, NO_2^-, $NO_2^-H_2O$, and O_3^-. The reactions were found to proceed either via proton transfer, switching, or clustering. A new proton transfer channel leading to alkylperoxy carboxylate radicals ($R_{-H}(OO\cdot)COO^-$) was observed for propionic, butyric, and pinonic acids. (Int J Mass Spectrom 194 (2000) 53–68) © 2000 Elsevier Science B.V.

Keywords: Ion-molecule reactions; Carboxylic acids; Chemical ionisation; Tropospheric trace constituents

1. Introduction

Organic acids are important atmospheric trace gases. They contribute significantly to acidity of atmospheric condensed water and acid precipitation. As end products of the atmospheric oxidation of hydrocarbons they reflect the physicochemical history and oxidation capacity of an airmass. High-molecular-weight mono- and dicarboxylic acids are considered to have an important role in the formation of atmospheric secondary organic aerosol (SOA), especially above forests. Since organic aerosols largely contribute to the number concentration of total atmospheric aerosols and cloud condensation nuclei [1], organic acids may have a significant impact at least on local climate.

Sources of atmospheric organic acids include both natural and man-made as well as direct and indirect ones. Direct sources include emissions from the biosphere, biomass burning, and motor vehicle exhaust [2–4]. Secondary sources include photochemical oxidation of atmospheric hydrocarbons [5–7]. Sources of propionic acid (CH_3CH_2COOH) and butyric acid ($CH_3(CH_2)_2COOH$) are less well characterized than the sources of the more abundant formic and acetic acids. Propionic and butyric acids are expected to be formed via O_3 initiated oxidation of 1-butene and 1-pentene, respectively, and of some higher alkenes. Glyoxylic acid (HCOCOOH) and pyruvic acid ($CH_3COCOOH$), respectively, are α-oxocarboxylic acids that have the same molecular weights as propionic and butyric acids, respectively. Atmospheric

* Corresponding author.

[1] Permanent address: Department of Physics, P. O. Box 9, FIN-00014, University of Helsinki, Finland.

[2] Biogeochemistry division, Max-Planck-Institute for Chemistry, P.O. Box 3060, D-55020 Mainz, Germany.

PII S1387-3806(99)00172-4

sources of glyoxylic and pyruvic acids are not well established but photooxidation of aromatic hydrocarbons and 1,3-dienes are likely to play a role. Atmospheric oxidation of isoprene (2-methyl-1,3-butadiene) is considered as a potential source of atmospheric pyruvic acid [3,8]. Isoprene is the most abundant natural hydrocarbon emitted mainly by deciduous trees [9]. Pinonic acid (2,2-dimethyl-3-acetylcyclobutylethanoic acid) is formed via O_3 initiated oxidation of α-pinene [10–12], the most abundant monoterpene emitted mainly by coniferous trees [9]. In addition to O_3, reactions of OH radical with propanal, butanal, glyoxal, and pinonaldehyde, respectively, also apparently lead to formation of propionic, butyric, glyoxylic, and pinonic acids, respectively. Peroxy acyl radicals ($RC(O)O_2$) are key intermediates in these reactions [13,14].

Gas-phase concentrations of higher carboxylic acids ($\geq C_3$) have seldom been reported. Propionic, butyric, and pyruvic acids have been sampled from the atmosphere by filter-, mist chamber, cryogenic trapping, and denuder methods and analysed by ion chromatography [3,15–18]. Glyoxylic acid and also pyruvic acid have been sampled with a glass coil scrubber and analysed as 2,4-dinitrophenylhydrazine (DNPH) derivatives with high-performance liquid chromatography (HPLC) [8]. Gaseous pinonic acid has been determined indirectly by simultaneously measuring the concentration of the acid in particle phase and the total (gas + particle phase) acid concentration. A denuder was used to eliminate the gaseous acid. The acid was sampled with filters and polyurethane foam plugs and analysed by gas chromatography mass spectrometry (GC-MS) [19].

From previous atmospheric measurements it was found that propionic acid is often, after formic and acetic acids (HCOOH, CH_3COOH), the most abundant organic acid in the urban atmosphere. Measured atmospheric volume mixing ratios of propionic acid range between some tens of ppt (parts per trillion) to ~1 ppb (parts per billion) [15–18]. Up to few hundred parts per trillion of pyruvic acid have been detected in forested environments in the summertime [3,8,20]. To our knowledge, gas-phase concentrations of glyoxylic acid and pinonic acid have been reported only once. Surprisingly high concentrations from a few hundred parts per trillion up to a few parts per billion of glyoxylic acid were observed [8]. As expected, low concentrations of pinonic acid at sub-parts-per-trillion range were measured [19]. Time resolution in the latter study was 6 h.

Propionic, butyric, glyoxylic, and pyruvic acids are likely to be present in atmospheric condensed water due to their substantial solubility in water. Indeed wet and dry deposition are considered as major sinks of these acidic trace gases [16,20]. There is considerable evidence that pinonic acid, pinic acid (3-carboxy-2,2-dimethylcyclobutylacetic acid), and other acidic high-molecular-weight ($\geq C_8$) monoterpene oxidation products, may under some conditions, be important gaseous precursors of new particles above forests. This has been suggested based on laboratory studies [8,9,21–23], and recent field studies support the suggestion [19,24].

This article reports on laboratory measurements of gas-phase reactions of negative ions with propionic, butyric, glyoxylic, pyruvic, and pinonic acids. These measurements provide a base for the detection of these acidic trace gases using ion molecule reaction mass spectrometry (IMRMS).

2. Experimental

The present laboratory experiments were performed at 1.5 and 9 hPa using a flow tube ion reactor with a quadrupole mass spectrometer (QMS) for ion analysis and detection. Qualitative studies were also performed at 40 hPa using a modified commercial Finnigan (San Jose, CA) ion trap mass spectrometer as a detector. The flow reactor consisted of a stainless steel flow tube (i.d. 4 cm) with an ion source and inlet ports for addition of reactant gases and water vapour. The same experimental setup has been used in our previous investigations of ion molecule reactions of formic and acetic acids [25] and is described in detail elsewhere [26,27].

Briefly, the experiments were performed at 1.5 and 9 hPa, respectively, in a laminar buffer gas (N_2 + O_2) flow of 5.5 and 11 standard liters per minute (slm) at

standard temperature and pressure, respectively. At a flow reactor pressure of 1.5 hPa the bulk flow velocity was ~50 m/s. O_2^- and O_3^- ions were produced by a capillary tube ion source (CIS) using a 2 slm O_2 source gas flow. A detailed description of the ion source and of the reactant ion evolution has been given previously [26]. For the generation of the reactant ion CO_3^- or the reactant ions NO_3^- and NO_2^- small amounts of CO_2 or NO_2 were introduced into the source gas flow. In addition to the more abundant ions, the ion source also produced less abundant ions, particularly CO_4^-, HCO_3^-, and HCO_4^-. To achieve low $[O_2]$ conditions, CO_3^- was also produced by introducing 1–2 slm Ar and small amounts of CO_2 into the CIS. Hydrated reactant ions $X^-(H_2O)_n$ were produced by introducing water vapour into the flow reactor, from a water reservoir located downstream of the CIS.

Known fluxes of propionic and butyric acids were generated by a permeation source (Kin-Tek Laboratories, La Marque, TX). Acid vapour diffusing from the permeation source was diluted with a nitrogen gas flow, which was passed through the permeation source at atmospheric pressure. The acids were added to the flow reactor downstream of the ion source through a Teflon tube inlet with a critical orifice. The flow through the critical orifice fabricated from stainless steel was 0.85 slm. The remainder of the permeation source flow was discarded. Acid concentrations in the flow reactor were calculated from the gas flows, the flow reactor pressure, and the known emission rates of the permeation tubes. The concentration of the acid was changed by varying the temperature of the permeation source in steps of 5 or 10 K and by allowing the source to stabilise thermally for at least 30 min. Glyoxylic, pyruvic, and pinonic acids were introduced into the flow tube by vaporising solid glyoxylic or pinonic acid or liquid pyruvic acid. With this method, no quantification of the concentrations of these acids in the flow tube was possible.

The mass discrimination of the quadrupole instrument was determined from integral spectra and by fitting the product ion yields to equal the amount of reacted reactant ions for those reactions, which produced only one distinct product ion species. The residence time t_R of the ions between the acid inlet and the quadrupole mass spectrometer was measured by pulsing the ion swarm with a repeller grid. For the 1.5 and 9 hPa measurements residence times of 10.5 ± 0.5 and 32 ± 1 ms, respectively, were measured.

In the presence of water vapour in the flow reactor, a rapid ion hydration equilibrium was established. The ion hydration equilibrium was also maintained when reactant acid was added, even in those cases where the reactivities of the different hydrates with the acid were different [25]. Since in most cases several ion hydrates existed simultaneously, an effective reaction rate coefficient k_{eff}; being a weighted sum of the individual reaction rate coefficients k_i of the individual hydrates, was measured. From the measured k_{eff}, the reaction rate coefficients of the individual hydrates were determined as described in our earlier publication [25].

Carboxylic acids are known for their ability to dimerize efficiently. This can cause problems in the determination of reaction rate coefficients and reaction channels for monomers if dimer concentrations are significant [25]. Beyond propionic acid the strength of dimer hydrogen bonding remains essentially constant [28] and the concentration of butyric acid dimers can be approximated based on the equilibrium constant of propionic acid. Using the value of Taylor and Bruton [28] we calculate that under the present experimental conditions <15% of propionic and butyric acids was in the dimer form in the permeation source flow (at atmospheric pressure). When the acid entered the low pressure flow reactor, it was diluted and rapidly attained a new equilibrium with respect to dimerisation [29,30]. Under the conditions in the flow reactor <0.005% of propionic and butyric acid molecules were in the dimer form, if the equilibrium constants are assumed to be pressure independent.

3. Results

3.1. $CO_3^-(H_2O)_{0,1,2}$ reactions

Fig. 1 shows product ion spectra obtained with the QMS for the reactions of CO_3^- reactant ions with

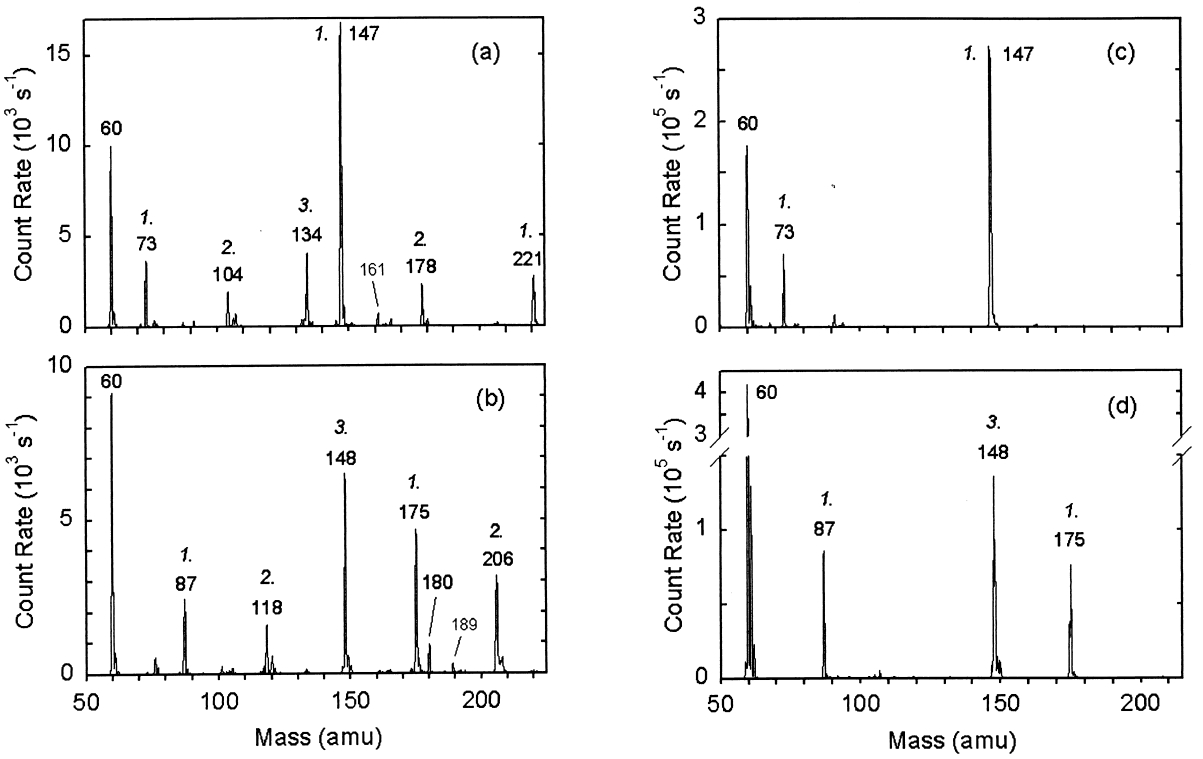

Fig. 1. Ion mass spectra of the reactions of CO_3^- (60 u) with (a) propionic acid (CH_3CH_2COOH), (b) butyric acid ($CH_3(CH_2)_2COOH$), (c) glyoxylic acid (CHOCOOH), and (d) pyruvic acid ($CH_3COCOOH$) at 9 hPa. Three main product ion families are observed for propionic and butyric acids. The product ion families are (in u): *1*. $RCOO^-(RCOOH)_n$ (73, 147, 221 and 87, 175); *2*. $R_{-H}(OO\cdot)COO^-(RCOOH)_n$ (104, 178 and 118, 206); and *3*. $CO_3^-(RCOOH)_n$ (134 and 148). Product ions of glyoxylic and pyruvic acids, respectively, have the same mass numbers and belong to the same ion families as the product ions of propionic and butyric acids, respectively, but fewer product ion families are observed for the α-oxocarboxylic acids than for the monocarboxylic acids.

propionic (CH_3CH_2COOH), butyric ($CH_3(CH_2)_2COOH$), glyoxylic (HCOCOOH), and pyruvic ($CH_3COCOOH$) acids. Three dominant families of product ions are observed for propionic and butyric acids (RCOOH, R = CH_3CH_2 for propionic acid, and R = $CH_3(CH_2)_2$ for butyric acid): carboxylates $RCOO^-$, alkylperoxy carboxylate radicals $R_{-H}(OO\cdot)COO^-$, and CO_3^-RCOOH cluster ions. ($R_{-H}(OO\cdot)$ denotes that a hydrogen atom H in the alkyl chain R has been displaced by a peroxy group). In addition to these dominant product ions, less abundant product ions are also observed. These less abundant product ions will be discussed later. Reactions of glyoxylic acid produced only ions with $HCOCOO^-$ core ions [Fig. 1(c)]. Reactions of pyruvic acid produced only ions with CH_3COCOO^- and $CO_3^-CH_3COCOOH$ core ions [Fig. 1(d)]. Further reactions of $RCOO^-$, $R_{-H}(OO\cdot)COO^-$, and CO_3^-RCOOH with the acids produced higher cluster ions of the form $RCOO^-(RCOOH)_n$, $R_{-H}(OO\cdot)COO^-(RCOOH)_n$, and $CO_3^-(RCOOH)_n$. Cluster ions with n up to 2 were observed for propionic acid. For butyric acid only clusters up to $n = 1$ could be observed due to the restricted mass range of the QMS.

When the concentration of O_2 in the flow tube was minimized, $R_{-H}(OO\cdot)COO^-$ ions disappeared. Instead, new ions of the form $\dot{R}_{-H}COO^-$ appeared. At long reaction times (32 ms) and high educt conversions (Fig. 1) small amounts of ions with mass numbers 17 (OH) less than $R_{-H}(OO\cdot)COO^-$ were observed, indicating that peroxy radical permutation

Table 1
Equilibrium constants of hydration of selected organic ions

Anion	$(K_{hydr})_{n,n-1}$ (atm^{-1})[a]		
	$n=1$	$n=2$	$n=3$
$HCOO^-(H_2O)_n$[b]	1.2×10^6	1×10^5	6×10^3
$CH_3CH_2COO^-(H_2O)_n$	1.3×10^6	1×10^5	5×10^3
$CH_3(CH_2)_2COO^-(H_2O)_n$	1.6×10^6	7×10^4	5×10^3
$CH_2(O_2\cdot)CH_2COO^-(H_2O)_n$[c]	3.3×10^5	1×10^4	
$CH_3CH(O_2\cdot)CH_2COO^-(H_2O)_n$[c]	4.0×10^5	7×10^3	
$CO_3^-CH_3COOH\cdot(H_2O)_n$[b]	2×10^3		
$CO_3^-CH_3CH_2COOH\cdot(H_2O)_n$	8×10^2		
$CO_3^-CH_3(CH_2)_2COOH\cdot(H_2O)_n$	4×10^2		
$NO_3^-HCOOH\cdot(H_2O)_n$[b]	1.5×10^3		
$NO_3^-CH_3COOH\cdot(H_2O)_n$[b]	2×10^3		
$NO_3^-CH_3CH_2COOH\cdot(H_2O)_n$	7×10^2		
$NO_3^-CH_3(CH_2)_2COOH\cdot(H_2O)_n$	6×10^2		

[a] All equlibrium constants have a relative error of ±50%.
[b] Based on the work described in Viidanoja et al. [25].
[c] Representative peroxy radical isomer. Isomeric structure has not been verified.

reactions [14] leading to formation of $R_{-2H}(=O)COO^-$ took place [e.g., ion masses 161 and 180 u in Figs. 1(a) and (b), respectively].

In the presence of water vapour reactions were observed for the hydrated ions similar to those of the bare ions. The $RCOO^-$ product ions exhibited a strong tendency for hydration. Equilibrium constants of hydration have been given for $RCOO^-(H_2O)_{0,1,2}$, $R_{-H}(OO\cdot)COO^-(H_2O)_{0,1}$, and CO_3^-RCOOH ions in Table 1.

Due to the limited mass range of the QMS (<250 u), the reactions of pinonic acid were studied using a Paul Ion Trap Mass Spectrometer (PITMAS) [31]. The PITMAS has a much higher mass range (up to 2000 u) and also offers the possibility of *n*th generation fragmentation studies using the MS^n mode of the PITMAS. In the PITMAS ions are accumulated for times up to 8 s. In order to stabilise the ion trajectories in the ion trap, the ion trap is filled with a He bath gas at a pressure of 1 mTorr. The ions collide with the He atoms and are thereby kinetically cooled, thus stabilizing their trajectories. This is different from the operation of a linear quadrupole mass spectrometer, where the ions pass through the quadrupole system without collisions. These differences in the operation of a linear quadrupole system and an ion trap system have to be taken into account when interpreting ion spectra obtained with the two different instruments.

Fig. 2 shows ion mass spectra obtained for propionic, butyric, and pinonic acids with the PITMAS at 40 hPa. $RCOO^-(RCOOH)_n$ and $R_{-H}(OO\cdot)COO^-(RCOOH)_n$ ions with *n* up to 1 were observed for each acid. No CO_3^-RCOOH cluster ions could be observed. These observations evidently reflect the relative collisional stability of the ion families: CO_3^-RCOOH cluster ions are easily collisionally dissociated by the buffer gas within the ion optics and the quadrupole ion trap, but $RCOO^-RCOOH$ and $R_{-H}(OO\cdot)COO^-RCOOH$ cluster ions are bound stronger. Also, ions with mass numbers equal to "CO_5^-RCOOH" were observed for propionic, butyric, and pinonic acids with the PITMAS (166, 180, and 276 u, respectively) and in lesser amounts with the QMS at 9 hPa (but not at 1.5 hPa).

Product ions of the reaction of pinonic acid with CO_3^- were studied further by fragmenting them using the MS^n mode of the PITMAS. Fig. 3 shows MS^2 spectra of pinonate (183 u) and alkylperoxy pinonate radicals (214 u) with suggested structural formulas for the fragment ions. "CO_5^-RCOOH" ion of pinonic acid (276 u) could not be isolated with the PITMAS for MS^2 studies.

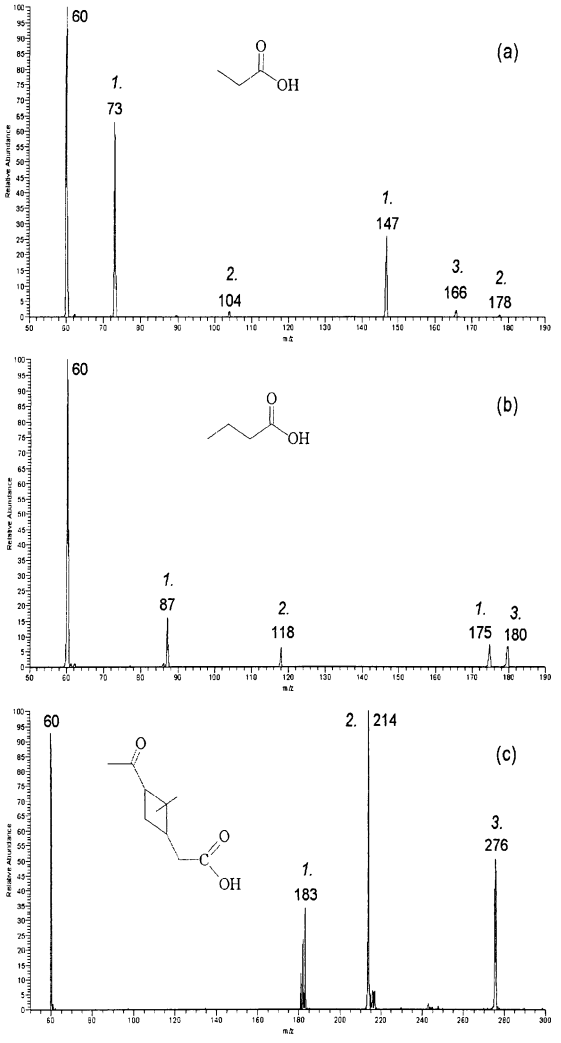

Fig. 2. Ion trap mass spectra of the reactions of CO_3^- (60 u) with (a) propionic acid, (b) butyric acid, and (c) pinonic acid at 40 hPa. Three product ion families are observed for propionic, butyric, and pinonic acids, respectively, in parentheses (u): *1.* $RCOO^-(RCOOH)_n$ (73, 147 and 87, 175 and 183); *2.* $R_{-H}(OO\cdot)COO^-(RCOOH)_n$ (104, 178 and 118 and 214); and *3.* ions tentatively identified as $CO_3^-R_{-H}(OOH)COOH$ (166 and 180 and 276).

3.2. $NO_3^-(H_2O)_{0,1,2}$ and $NO_2^-(H_2O)_{0,1,2}$ reactions

In contrast to CO_3^-, the reaction of NO_3^- with propionic, butyric, glyoxylic, and pyruvic acids, respectively, proceeds solely by a three body addition reaction leading to the $NO_3^-CH_3CH_2COOH$, $NO_3^-CH_3(CH_2)_2COOH$, $NO_3^-HCOCOOH$, and $NO_3^-CH_3COCOOH$ cluster ions, respectively. This is evident since the proton affinity of NO_3^- is much lower than that of $CH_3CH_2COO^-$, $CH_3(CH_2)_2COO^-$, and CH_3COCOO^- (Table 2). Because of structural similarity between glyoxylic and pyruvic acids, the proton affinity of glyoxylic acid is undoubtedly similar to that of pyruvic acid. Therefore, no proton

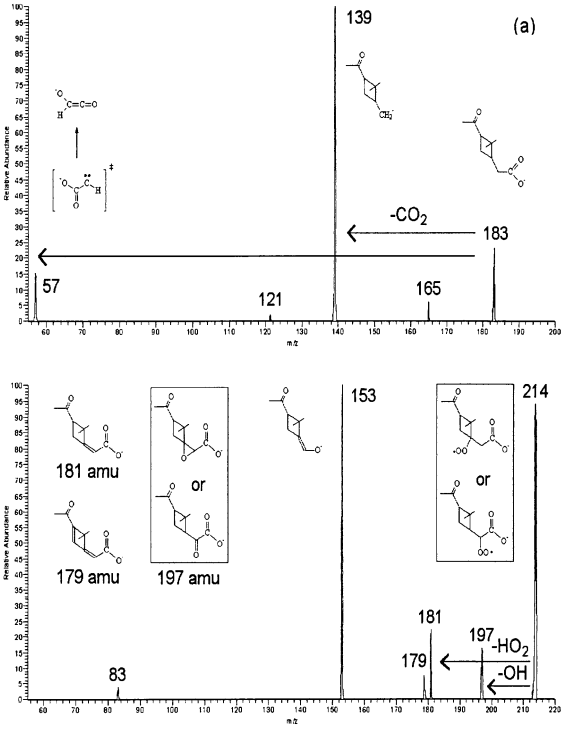

Fig. 3. MS^2 spectra of (a) pinonate (183 u) and (b) alkylperoxy pinonate radicals (214 u), the product ions of pinonic acid + CO_3^- reaction. Excitation (tickle) voltages of 0.65 and 0.5 V, respectively, were applied on the parent molecules for 30 ms.

Table 2
Proton affinities (PA) of selected anions [32]

Anion	PA (X^-) (kJ mol^{-1})
CH_3COO^-	1459
$CH_3CH_2COO^-$	1454
$CH_3(CH_2)_2COO^-$	1450
$HCOO^-$	1445
NO_2^-	1421
CH_3COCOO^-	1395
NO_3^-	1358

transfer from the acids to NO_3^- can occur. The same argument is true for NO_2^- in the case of propionic and butyric acids, where the only products observed were cluster ions $NO_2^-CH_3CH_2COOH$ and $NO_2^-CH_3(CH_2)_2COOH$. The reactions of NO_2^- with glyoxylic and pyruvic acids proceed both by proton transfer and clustering reactions leading to the $HCOCOO^-$, CH_3COCOO^-, $NO_2^-HCOCOOH$, and $NO_2^-CH_3COCOOH$. This is expected because the proton affinity of NO_2^- is higher than that of CH_3COCOO^- (Table 2). Secondary reactions of $NO_3^-(RCOOH)$ and $NO_2^-(RCOOH)$ cluster ions producing the higher order cluster ions $NO_3^-(RCOOH)_2$ and $NO_2^-(RCOOH)_2$ were also observed. Similar reactions as in the case of the bare ions were observed if water was added. Equilibrium constants of hydration have been given for $NO_3^-CH_3CH_2COOH$ and $NO_3^-CH_3(CH_2)_2COOH$ ions in Table 1.

4. Discussion

The present studies are a sequel to our studies on negative ion molecule reactions of formic and acetic acids, and the reader is encouraged to review the earlier work [25] for further information.

In the case of O_3^- reactant ions only proton transfer products were observed in the reactions with propionic and butyric acids:

$$O_3^- + RCOOH \rightarrow RCOO^- + \text{products} \quad (1)$$

When the concentration of the acids is increased, the count rate of the O_3^- reactant ions decreases exponentially (Fig. 4). An exponential decrease is expected for a pseudo-first-order-reaction-like reaction [Eq. (1)].

In these cases the reaction rate coefficients were determined from the linear decrease of the logarithm of the count rate with increasing acid concentration. By contrast, the reactions producing cluster ions CO_3^-RCOOH, NO_3^-RCOOH, and NO_2^-RCOOH exhibited deviations from exponential behaviour at higher [product ion]/[reactant ion] ratios. This was expected because we found out in our earlier studies

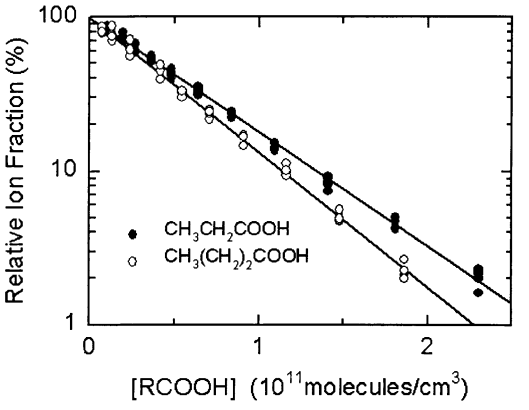

Fig. 4. Reactant ions vs. the concentration of propionic and butyric acids for the reactions of propionic (CH_3CH_2COOH) and butyric ($CH_3(CH_2)_2COOH$) acids with O_3^- at 1.5 hPa.

of the ion molecule reactions of formic and acetic acids that the cluster ions of CO_3^-, NO_3^-, and NO_2^- are thermally unstable and they decompose back to the reactants [25]. In these cases the forward reaction rate coefficients were determined from the exponential decrease of the reactant ion count rate at low reactant conversion. The reaction rate coefficients for the reactions of propionic and butyric acid with CO_3^-, O_3^-, NO_3^-, and NO_2^- reactant ions are given in Table 3.

Other possible reasons for the nonexponential decrease of reactant ions in the cases where cluster products were observed may include: (1) electric field induced collisional dissociation (ECD) of cluster ions behind the inlet orifice of the mass spectrometer, and (2) reactions of monocarboxylic acid dimers [25].

These possibilities have been discussed in our previous study on formic and acetic acid reactions and they could be ruled out. Similar considerations apply to the present study, so that the thermal decomposition of cluster ions remains as the most likely reason for the observed nonexponential behaviour also in the case of propionic and butyric acids.

Thermal (collisional) instability of CO_3^-RCOOH, NO_3^-RCOOH, and NO_2^-RCOOH cluster ions is further supported by the observation that $RCOO^-$, and $R_{-H}(OO\cdot)COO^-$ ions, but not the CO_3^-RCOOH cluster ions (of C_1–C_4 monocarboxylic acids and pinonic

Table 3
Ion molecule reactions of propionic and butyric acid with negative ions (p = 1.5 hPa, T = 293 ± 3 K)

Reaction			k_{meas}[a]	k_{coll}[b]
CO_3^- + CH_3CH_2COOH	→	Products[c]	11[d]	19
$CO_3^-(H_2O)$ + CH_3CH_2COOH	→	Products[c]	19[e]	17
O_3^- + CH_3CH_2COOH	→	$CH_3CH_2COO^-$ + Products	17	20
NO_3^- + CH_3CH_2COOH + M	→	$NO_3^-CH_3CH_2COOH$ + M	10[d]	19
$NO_3^-(H_2O)$ + CH_3CH_2COOH	→	$NO_3^-CH_3CH_2COOH$ + H_2O	19[f]	17
NO_2^- + CH_3CH_2COOH + M	→	$NO_2^-CH_3CH_2COOH$ + M	18[d]	20
$NO_2^-(H_2O)$ + CH_3CH_2COOH	→	$NO_2^-CH_3CH_2COOH$ + H_2O	20[g]	18
CO_3^- + $CH_3(CH_2)_2COOH$	→	Products[c]	13[d]	
$CO_3^-(H_2O)$ + $CH_3(CH_2)_2COOH$	→	Products[c]	21[e]	
O_3^- + $CH_3(CH_2)_2COOH$	→	$CH_3(CH_2)_2COO^-$ + Products	19	
NO_3^- + $CH_3(CH_2)_2COOH$ + M	→	$NO_3^-CH_3(CH_2)_2COOH$ + M	11[d]	
$NO_3^-(H_2O)$ + $CH_3(CH_2)_2COOH$	→	$NO_3^-CH_3(CH_2)_2COOH$ + H_2O	19[f]	
NO_2^- + $CH_3(CH_2)_2COOH$ + M	→	$NO_2^-CH_3(CH_2)_2COOH$ + M	18[d]	
$NO_2^-(H_2O)$ + $CH_3(CH_2)_2COOH$	→	$NO_2^-CH_3(CH_2)_2COOH$ + H_2O	20[g]	

[a] Measured reaction rate coefficient; all rate coefficients are reported in units of 10^{-10} cm^3 molecule^{-1} s^{-1} and have a relative error of ±40%.
[b] Calculated collision rate coefficient (10^{-10} cm^3 molecule^{-1} s^{-1}); collision rate coefficients are calculated according to the theory of Su and Chesnavich [33].
[c] See Secs. 3.1 and 4 for details.
[d] Effective binary reaction rate coefficient at 1.5 hPa synthetic air.
[e] Effective rate coefficient for hydrate composition $CO_3^-(H_2O)_n$: 95% n = 1, 5% n = 2.
[f] Effective rate coefficient for hydrate composition $NO_3^-(H_2O)_n$: 90 n = 1, 10% n = 2.
[g] Effective rate coefficient for hydrate composition $NO_2^-(H_2O)_n$: 70% n = 1, 30% n = 2.

acid) can be detected by the PITMAS (Fig. 2). As discussed above, the collision frequency and residence time of the ions within the PITMAS is much higher than in the QMS. This is likely to lead to extensive decomposition of labile ions within the PITMAS.

Figs. 5 and 6 show the CO_3^- reactant ions and their product ions as a function of the propionic and butyric acid concentration, respectively, in the flow reactor. The reactant ion CO_3^- decreases with increasing concentration of the monocarboxylic acid (RCOOH). $RCOO^-$ and $R_{-H}(OO\cdot)COO^-$ ions and CO_3^-RCOOH cluster ions, respectively, are formed through proton transfer (PT) and clustering reactions, respectively.

To describe the observations in Figs. 5 and 6, we propose the following reaction scheme for propionic acid. For butyric acid analogous reactions are expected to take place:

$$CO_3^- + CH_3CH_2COOH \xrightarrow{M} CO_3^-CH_3CH_2COOH \quad (2)$$

$$\rightarrow CH_3CH_2COO^- + CO_2 + OH \quad (3a)$$

$$\rightarrow CH_3CH(\cdot)COO^- + CO_2 + H_2O \quad (3b)$$

$$CH_3CH(\cdot)COO^- + O_2 \xrightarrow{M} CH_3CH(O_2\cdot)COO^- \quad (4)$$

$$CO_3^-CH_3CH_2COOH \xrightarrow{M} CO_3^- + CH_3CH_2COOH \quad (5)$$

$$\xrightarrow{M} CH_3CH_2COO^- + CO_2 + OH \quad (6a)$$

$$\xrightarrow{M} CH_3CH(\cdot)COO^- + CO_2 + H_2O \quad (6b)$$

$$CO_3^-H_2O + CH_3CH_2COOH \rightarrow CO_3^-CH_3CH_2COOH + H_2O \quad (7)$$

$$\rightarrow CH_3CH_2COO^- + H_2O + CO_2 + OH \quad (8a)$$

$$\rightarrow CH_3CH(\cdot)COO^- + CO_2 + 2H_2O \quad (8b)$$

The initial reaction of CO_3^- with RCOOH may either lead to the cluster ion CO_3^- RCOOH [reaction (2)], or to one of the two proton transfer products $RCOO^-$ [reaction (3a)] or $\dot{R}_{-H}COO^-$ [reaction (3b)]. The $R_{-H}{\cdot}COO^-$ ion rapidly attaches O_2 to form the alkylperoxy carboxylate radicals $R_{-H}(OO\cdot)COO^-$. The cluster product CO_3^-RCOOH may thermally decompose, leading back to CO_3^- and RCOOH, or leading to the proton transfer products $RCOO^-$ [reaction (6a)] or $\dot{R}_{-H}COO^-$ [reaction (6b)]. For hydrated CO_3^-, similar reactions as for the bare CO_3^- are expected to take place [reactions (7), (8a), and (8b)].

$RCOO^-$ and $R_{-H}(OO\cdot)COO^-$ product ions of

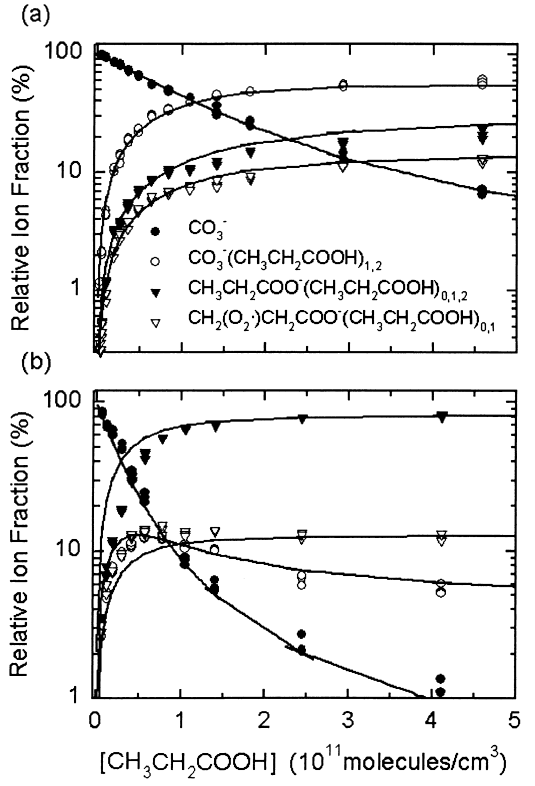

Fig. 5. Reactant and product ions vs. the concentration of propionic acid for the reaction of propionic acid with bare CO_3^- (a) at 1.5 hPa and (b) at 9 hPa. Lines are calculations using rate coefficients given in Table 4 (D + CA). See the text for details.

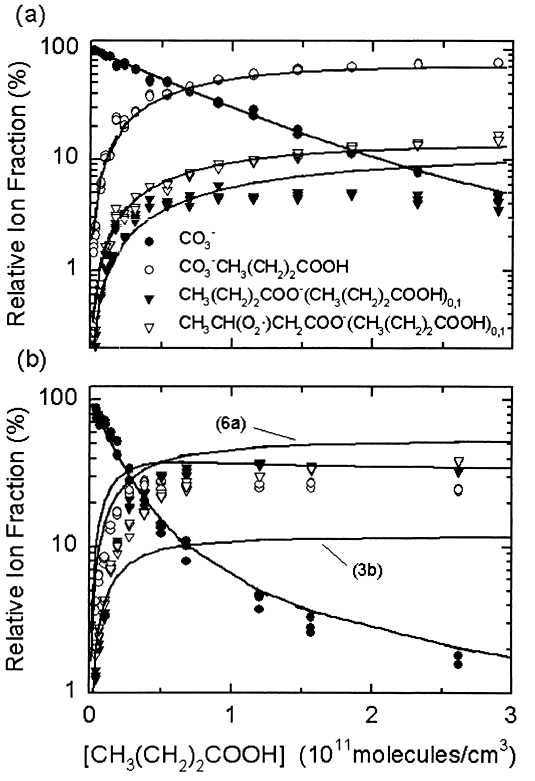

Fig. 6. Reactant and product ions vs. the concentration of butyric acid for the reaction of butyric acid with bare CO_3^- (a) at 1.5 hPa and (b) at 9 hPa. Lines are calculations using rate coefficients given in Table 4 (D + CA). See the text for details.

propionic acid may either form via direct proton transfer reactions (3) and (8) or via collisional activation of product cluster [reaction (6)]. CO_3^-RCOOH cluster ions are formed via clustering [reaction (2)] and switching [reaction (5)] reactions of bare and hydrated CO_3^- ions, respectively [25]. For butyric acid, reactions analogous to the reactions (2)–(8) of propionic acid can be written.

When O_2 in the flow reactor was replaced by argon, R_{-H}·COO^- ions were formed instead of $R_{-H}(OO\cdot)COO^-$. This clearly shows that the formation of $R_{-H}(OO\cdot)COO^-$ ions is a two step process where an oxygen molecule is, under O_2 rich conditions, instantly added [reaction (4)] to the alkyl R_{-H}·COO^- radical formed in reactions (3b), (8b), and/or (6b).

In principle, a hydrogen atom can be abstracted from two alkyl sites in propionate (CH_3CH_2–) and from three alkyl sites in butyrate ($CH_3CH_2CH_2$–). Abstraction of α hydrogen is energetically most likely since the reaction produces an anion with the most extensive charge delocalisation. Since the reactions of acetic acid did not produce $R_{-H}(OO\cdot)COO^-$ ions [25] it may be possible that abstraction from the CH_3– group is not energetically favourable, or that the reaction proceeds via a transition state that is not accessible for an α hydrogen.

Ions with mass numbers equal to CO_5^-RCOOH were also observed (Figs. 1 and 2). The formation rate of these ions increased with pressure and was not decreased by hydration of CO_3^-. These ions were stable enough to be detected by PITMAS but CO_3^-RCOOH ions were not (Fig. 2), nor could "CO_5^-RCOOH" ions be isolated for CID studies by PITMAS. Ions with the structural formula of CO_3^-RCOOH·O_2 are likely to be less stable than the CO_3^-RCOOH ions. Yields of both "CO_5^-RCOOH" and $R_{-H}(OO\cdot)COO^-$ ions increase with chain length of carboxylic acid. The yields of these ions also increase with pressure. We suggest that "CO_5^-RCOOH" ions are in fact parallel products of $R_{-H}(OO\cdot)COO^-$ and have a structural formula of $CO_3^-R_{-H}(OOH)COOH$.

Figs. 7(a)–(c) show the bare and hydrated CO_3^- reactant ions, the sum of proton transfer (PT) product ions, and CO_3^-RCOOH cluster product ions as function of the propionic acid (CH_3CH_2COOH) concentration in the flow reactor at 1.5 and 9 hPa. PT product

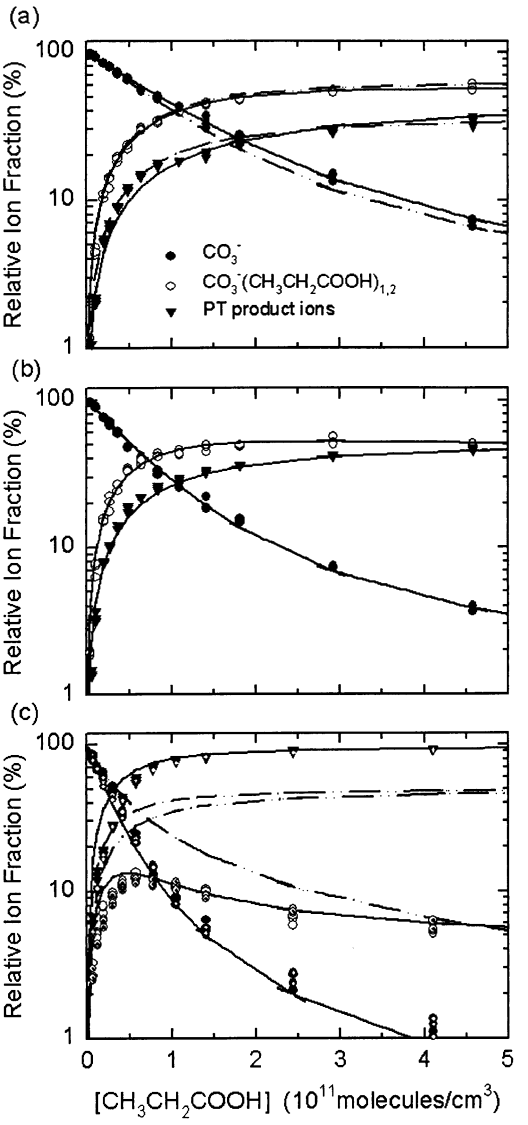

Fig. 7. Reactant ions, $CO_3^-(CH_3CH_2COOH)_{1,2}$ and proton transfer (PT) product ions vs. the concentration of propionic acid for the reaction of propionic acid with (a) bare CO_3^- at 1.5 hPa, (b) hydrated CO_3^- at 1.5 hPa, and (c) bare (undotted circles) and hydrated (dotted circles) CO_3^- at 9 hPa. Lines are calculations using rate coefficients given in Table 4. Proton transfer channels considered in the calculations: Direct (D; dash-dot-dot) and collisional activation (CA; solid).

Table 4
Calculated reaction rate coefficients for the reactions of propionic and butyric acids with CO_3^- at 1.5 and 9 hPa considering different proton transfer reaction mechanisms

	Propionic acid						Butyric acid					
Acid	1.5			9			1.5			9		
P/hPa PT[a]	D[d]	CA[d,e]	D + CA[f]	D[g]	CA[g]	D + CA[h]	D	CA	D + CA[i]	D	CA	D + CA[j]
k_2[b]	8	11	9	15.5	19	17	11	13	11.4	18.5	21	17
k_3[b]	3	0	1.2	3	0	1.2	2.5	0	1.6	2.5	0	1.6
k_5[c]	50	50	50	100	100	100	18	18	18	30	30	30
k_6[c]	0	60	45	0	100	90	0	40	15	0	55	30
k_7[b]		19			19			21			21	

[a] Proton transfer (PT) mechanism considered: PT occurs only via direct (D) reactions [(3a) + (3b)], PT occurs only via collisional activation (CA) reactions [(6a) + (6b)], or via reactions (3b) and (8a) (D +CA).
[b] Binary reaction rate coefficient (10^{-10} cm^3 $molecules^{-1}$ s^{-1}).
[c] Thermal decomposition rate coefficient (molecules/s).
Fittings shown in: [d]Fig. 7(a), [e]Fig. 7(b), [f]Fig. 5(a), [g]Fig. 7(c), [h]Fig. 5(b), [i]Fig. 6(a), and [j]Fig. 6(b).

ions include the ions with $RCOO^-$ and $R_{-H}(OO\cdot)COO^-$ core ions. Similar graphs were drawn for butyric acid. Since the observations made for butyric acid were qualitatively identical to those of propionic acid the figures of propionic acid are applied here to illustrate both acids.

At 9 hPa bare CO_3^- and hydrated CO_3^- showed identical decay curves [Fig. 7(c)]. Also the product ions of bare and hydrated CO_3^- ions showed the same growth curves. Because the reaction of hydrated CO_3^- with propionic acid is a fast reaction occurring at the collision rate (Table 3), this indicates that the reaction of bare CO_3^- with propionic acid also is close to the collision rate and must therefore be at or close to its high pressure limit. Therefore, also, the thermal decomposition of CO_3^-RCOOH cluster ions [reactions (5) and (6)] must be close to the high pressure limit. Because the yield of PT product ions was similar for bare and hydrated CO_3^- the rate of PT reactions is not affected by water. Thus, if direct PT reactions of bare and hydrated CO_3^- ions [reactions (3) and (8)] are important reaction channels for propionic and butyric acids, then the reaction rate coefficients of these reactions must be similar.

At 1.5 hPa bare CO_3^- [Fig. 7(a)] shows slower decay rates than hydrated CO_3^- [Fig. 7(b)]. This indicates that at 1.5 hPa the clustering reaction (2) has not reached its high pressure limit yet. The overall consumption of CO_3^- is therefore smaller than in the case of $CO_3^-H_2O$, where the switching reaction (7) is a fast and pressure independent two body reaction.

Although the switching reaction of hydrated CO_3^- [reaction (7)] is pressure independent, the yield of CO_3^-RCOOH is much higher at 1.5 hPa than at 9 hPa. This observation is consistent with an expected pressure dependent thermal decomposition [reaction (5)]. The rate of the thermal decomposition reaction (5) increases with increasing pressure, leading to a decreasing yield of the cluster product CO_3^-RCOOH.

The relative contributions of the PT channels [reactions (3), (6), and (8)] and the clustering channels [reactions (2) and (5)] for the bare and the hydrated case were determined by fitting the reaction kinetics of reactions (2)–(8) to the measured product ion distributions. At the first stage PT products were fitted using either only a direct [reactions (3) and (8)] or only collisional activation [reaction (6)] channel and omitting the other. A similar pressure dependency was expected and used for pressure dependent reaction channels (2), (5), and (6) between 1.5 and 9 hPa. The results are summarised in Table 4 (D and CA).

At 1.5 hPa the total forward reaction rates were determined from the exponential decrease of the reactant ion count rate at low reactant conversion. When the direct PT reactions (3) and (8) were considered (D and D + CA in Table 4) the relative contributions of the direct reaction channels [reactions (2), (3), (7), and (8)] to the total forward reaction rate

Table 5
Equilibrium constants for selected cluster forming reactions ($T = 293 \pm 3$ K)

Reaction			K_{eq} (atm^{-1})	ΔG^0_{293} (kcal mol^{-1})
CO_3^- + CH_3COOH + M	↔	$CO_3^-CH_3COOH$ + M	2.6×10^8 (±50%)[a]	−11.3 (±0.2)[a]
NO_3^- + HCOOH + M	↔	NO_3^-HCOOH + M	3.2×10^8 (±50%)[a]	−11.4 (±0.2)[a]
NO_3^- + CH_3COOH + M	↔	$NO_3^-CH_3COOH$ + M	5.7×10^8 (±50%)[a]	−11.8 (±0.2)[a]
NO_3^- + CH_3CH_2COOH + M	↔	$NO_3^-CH_3CH_2COOH$ + M	9.1×10^8 (±50%)	−12.0 (±0.2)
NO_3^- + $CH_3(CH_2)_2COOH$ + M	↔	$NO_3^-CH_3(CH_2)_2COOH$ + M	3.9×10^9 (±50%)	−12.8 (5)(±0.2)
NO_2^- + CH_3COOH + M	↔	$NO_2^-CH_3COOH$ + M	1.2×10^9 (±50%)[a]	−12.2 (±0.2)[a]
NO_2^- + CH_3CH_2COOH + M	↔	$NO_2^-CH_3CH_2COOH$ + M	2.2×10^9 (±50%)	−12.5 (±0.2)
NO_2^- + $CH_3(CH_2)_2COOH$ + M	↔	$NO_2^-CH_3(CH_2)_2COOH$ + M	9.0×10^9 (±50%)	−13.3 (±0.2)

[a] Adopted from Viidanoja et al. [25].

were determined by extrapolating the relative product yields to zero acid concentration. The same pressure independent PT reaction rate coefficients were then applied at 9 hPa.

The lines in Figs. 7(a)–(c) are calculations using the reaction rate coefficients given in Table 4. At 1.5 hPa the observed product ion distributions of propionic and butyric acid can be explained by both direct and collisional activation PT reactions. However, at 9 hPa the direct reactions (3) and (8) are too slow to account for the observed product yields [dash-dot-dot in Fig. 7(c)], but good agreement is still observed between the measured data and calculated values (solid lines in Fig. 7(c)] if all PT products are assumed to be formed via collisional activation PT reactions (6). Good agreement is still achieved for both acids if a minor part of PT products ($\sim$1–2 $\times$ 10^{-10} cm^3 $molecules^{-1}$ s^{-1}) is assumed to be formed via the direct reactions (3) and (8).

For propionic acid the ratio of PT product ions $RCOO^-/R_{-H}(OO\cdot)COO^-$ increases with pressure [Figs. 5(a) and (b)]. Because the pressure dependency of the rates of the reactions (6a) and (6b) is likely to be similar between 1.5 and 9 hPa, no pressure dependence of the PT product ion ratio is expected if the PT products are formed via these reactions. Thus, the formation of $R_{-H}(OO\cdot)COO^-$ ions via reactions (3b) and (8b) seems likely. For propionic acid good agreement is achieved between measured data and calculations if all of the $R_{-H}(OO\cdot)COO^-$ ions are assumed to be formed via pressure independent direct PT reactions (3b) and (8b) and all of the $RCOO^-$ ions are assumed to be formed via pressure dependent collisional activation [reaction (6a)]. Calculations for bare CO_3^- at 1.5 and 9 hPa, respectively, are shown with lines in Figs. 5(a) and (b), respectively. Reaction rate coefficients are summarised in Table 4 (D + CA). The same treatment underestimated the $R_{-H}(OO\cdot)COO^-$ ions of butyric acid at 9 hPa [Fig. 6(b)]. This suggests that at least a part of $R_{-H}(OO\cdot)COO^-$ ions of butyric acid may be formed via reaction (8b). Since $RCOO^-(RCOOH)_2$ of butyric acid and $R_{-H}(OO\cdot)COO^-(RCOOH)_2$ of propionic and butyric acid were beyond the mass range of the QMS, further analysis of the reaction mechanisms was not possible and some uncertainty and considerable uncertainty, respectively, remains in the interpretation of the reaction mechanisms of propionic acid and butyric acid, respectively.

The pure cluster forming reactions of bare and hydrated NO_3^- and NO_2^- with propionic and butyric acids were also analysed in terms of thermal decomposition reactions. From the ratios of the reaction rate coefficients for the forward and thermal decomposition reactions, equilibrium constants were obtained. The equilibrium constants are summarised in Table 5. Table 5 also gives the free energy changes for T = 293 K, ΔG^0_{293}, calculated from the equilibrium constants using the relation $\Delta G^0_{293} = -RT \ln(K_{eq})$.

5. Comparison between carboxylic acids

In this and the previous paper [25] we have performed quantitative studies of the negative ion molecule reactions of monocarboxylic acids, formic

(HCOOH), acetic (CH_3COOH), propionic (CH_3CH_2COOH), and butyric ($CH_3(CH_2)_2COOH$) acids. Qualitatively, we have also studied reactions of the α-oxocarboxylic acids, glyoxylic (HCOCOOH), and pyruvic ($CH_3COCOOH$) acids and the ϵ-ketocarboxylic acid, pinonic acid. Several trends can be observed when the characteristics of the ion molecule reactions are compared. The following properties of the ion molecule reactions increase systematically with increasing alkyl chain length of the monocarboxylic acid: (1) The complexity of CO_3^- and $CO_3^-(H_2O)$ reactions; (2) the equilibrium constants for cluster forming reactions of CO_3^-, NO_3^-, and NO_2^- reactant ions (Table 5); and (3) the reaction rate coefficients for the reactions with CO_3^-, O_3^-, NO_3^-, and NO_2^- ions (Table 3 and Tables 2 and 3 in [25]).

These observations can be explained by properties of the excited complexes formed by clustering [e.g., reaction (2)] or collisional activation [e.g., reactions (5) and (6)]. The lifetime of the excited complex increases with increasing number of degrees of freedom. Thus also the probability that at a certain pressure the excited cluster intermediate is stabilised by a collision increases with increasing size of the acid. This is seen as higher forward reaction rates for clustering reactions and higher stability of cluster product ions for higher acids. The probability of rearrangements increases with increasing lifetime of the excited complex. This increases the probability of more complex reactions like the formation of alkylperoxy carboxylate radicals. This is reflected in the observations that the $[R_{-H}(OO\cdot)COO^-]/[RCOO^- + R_{-H}(OO\cdot)COO^-]$ ratio and the yield of tentatively identified $CO_3^-R_{-H}(OOH)COOH$ increase with the size of the carboxylic acid [cf. Fig. (2)].

The hydration tendency of $CH_3COO^-(H_2O)_n$ could not be determined quantitatively in our earlier experiments [25] because of interfering $HCO_4^-(H_2O)_n$ ions. The results of both studies show, however, that the hydration tendency of $RCOO^-(H_2O)_n$ does not depend on the length of the alkyl chain R for C_1–C_4 monocarboxylic acids (Table 1). The hydration tendency of different types of product ions decreases in the order of: $RCOO^- > R_{-H}(OO\cdot)COO^- > CO_3^-RCOOH \approx NO_3^-RCOOH$.

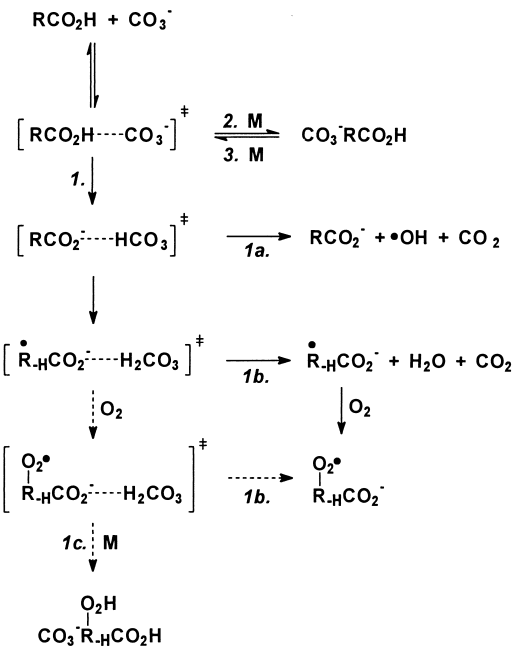

Fig. 8. Generalised reaction mechanism for the reactions of CO_3^- with carboxylic acids. M is an inert collision partner. $_{-H}$ indicates that a hydrogen atom has been abstracted from an alkyl group.

A generalised reaction mechanism for the reactions of the carboxylic acids with CO_3^- is given in Fig. 8. Whereas HCOOH and HCOCOOH reacted with $CO_3^-(H_2O)_n$ only in proton transfer reaction (*1* in Fig. 8) reactions of CH_3COOH, CH_3CH_2COOH, $CH_3(CH_2)_2COOH$, and $CH_3COCOOH$ proceeded also via clustering (*2*) and water ligand switching reactions. For CH_3CH_2COOH, $CH_3(CH_2)_2COOH$, and pinonic acid additional proton transfer channel(s) leading to $R_{-H}(OO\cdot)COO^-$ were observed (*1b*). CO_3^-RCOOH cluster ions (and NO_3^-RCOOH and NO_2^-RCOOH cluster ions) of the monocarboxylic acids were shown to be thermally unstable decomposing back to reactants (*3*).

Inability of HCOCOOH and $CH_3COCOOH$ to form $R_{-H}(OO\cdot)COO^-$ is at least partially due to the rigid structure of these molecules that evidently prevents the transition state leading to *1b* from forming.

Ions with mass numbers equal to "CO_5^-RCOOH" cluster ions were observed for CH_3CH_2COOH and $CH_3(CH_2)_2COOH$ and pinonic acid. At 40 hPa these

ions were among the most abundant product ions of pinonic acid [Fig. 4(c)]. The ions were tentatively identified as $CO_3^-R_{-H}(OOH)COOH$. We suggest that these ions are formed at high pressures via channel (*1c*) (Fig. 8).

Reaction products observed for pinonic acid were similar to those of CH_3CH_2COOH and $CH_3(CH_2)_2COOH$. CO_3^-RCOOH cluster ions of pinonic acid were too unstable to be observed with PITMAS. This suggests that the reaction mechanism of pinonic acid with CO_3^- is similar to that of CH_3CH_2COOH and $CH_3(CH_2)_2COOH$.

6. Application for atmospheric measurements by IMRMS

The ion molecule reactions of propionic, butyric, glyoxylic, pyruvic, and pinonic acids with negative ions described previously offer the possibility for sensitive in situ and real-time measurements of atmospheric concentrations of these acids. Reactions of bare and hydrated CO_3^- and NO_3^- ions have previously been used for the measurement of acidic trace gases like HNO_3, HCN, HF, HCOOH, CH_3COOH, and H_2SO_4 and other gases [25,34–39].

The higher stability of $RCOO^-(H_2O)_n$ and $R_{-H}(OO\cdot)COO^-(H_2O)_n$ product ions compared to that of $CO_3^-(RCOOH)_n$ and $NO_3^-(RCOOH)_n$ cluster ions makes these ions ideal for quantification of carboxylic acids at higher pressures and temperatures. The higher yields of $R_{-H}(OO\cdot)COO^-$ compared to $RCOO^-$ makes the former more suitable for the quantification of pinonic acid.

Because in the reactions of propionic, butyric, and pinonic acids the formation mechanism of $RCOO^-$ and $R_{-H}(OO\cdot)COO^-$ ions is rather complex and not fully understood yet, for atmospheric applications it is necessary to have an in-field calibration.

Several of the product ions of propionic and butyric acids, respectively, have the same mass numbers and belong to the same ion families as the product ions of glyoxylic and pyruvic acids, respectively. Thus, several of the product ions of ion molecule reactions of bare and hydrated CO_3^-, NO_3^-, and NO_2^- may not be used for unambiguous detection of these acidic trace gases unless fragmentation studies of the product ions are undertaken.

Unambiguous product ions for atmospheric measurements of propionic and butyric acids are the $R_{-H}(OO\cdot)COO^-(H_2O)_n$ ions from the reactions of bare and hydrated CO_3^-. Also CO_3^- CH_3CH_2COOH cluster ions (134 u) can be used for the quantification of propionic acid because glyoxylic acid does not form similar cluster ions [cf. Fig. 1(c)]. Proton transfer reactions of NO_2^- may offer a very selective, sensitive, and unambiguous method of detection for glyoxylic and pyruvic acids.

For a simple reaction obeying pseudo-first-order reaction kinetics and producing stable product ions, the concentration of an acid (HA) can be obtained from the reaction kinetics of a particular reaction using the measured ratio of product and reactant ions R, the reaction rate coefficient, k_{HA} for the reaction of the acid HA with the reactant ions, and the reaction time, t_R (cf. [40] and [41]):

$$[HA] = \frac{1}{k_{HA}t_R}\ln(1 + R) \tag{9}$$

For the ion molecule reactions investigated in this work, thermal decomposition reactions were observed in cases where cluster ions were formed. If the thermal decomposition to reactants is fast enough compared to the total reaction time, a steady state for the reactant ions (X^-) and the product cluster ions (X^-HA) establishes. In this case the acid concentration [HA] can be inferred from the steady state by [cf. 42]:

$$[HA] = K_{eq}^{-1}\frac{[X^-HA]}{[X^-]} \tag{10}$$

Equilibrium constants for several cluster forming reactions are given in Table 5. Equilibrium constant for the formation of $CO_3^-CH_3CH_2COOH$ cluster ions cannot, however, be applied in quantification of propionic acid, because a fast collisionally activated proton transfer channel exists:

$$CH_3CH_2COOH + CO_3^- \underset{k_{TD}}{\overset{k_C}{\rightleftharpoons}} CO_3^-CH_3CH_2COOH \xrightarrow{k_{CA}} \text{PT product ions} \quad (11)$$

k_C, k_{TD}, and k_{CA}, respectively, are clustering (or switching if CO_3^- is hydrated), thermal decomposition, and collisionally activated PT rate coefficients. If a pseudo-steady-state approximation can be applied to CO_3^-RCOOH, the reaction system (11) can be described by:

$$[CH_3CH_2COOH] = \left(\frac{k_{TD} + k_{CA}}{k_C}\right) \cdot \frac{[CO_3^-CH_3CH_2COOH]}{[CO_3^-]} \quad (12)$$

The steady state approximation can be applied for propionic acid if the reaction time t_R is sufficiently long and the $[CO_3^-CH_3CH_2COOH]/[CO_3^-]$ ratio is low. Fig. 9 shows the modelled quantity $[CO_3^-CH_3CH_2COOH]/[CO_3^-]$ plotted versus the propionic acid concentration at low atmospheric concentrations. The lines show calculations using the approximation of Eq. (12) and rate coefficients given in Table 4. The symbols are modelled values using the exact equation describing the full reaction system [reactions (2)–(6)]. Good agreement is observed between the modelled values (dots) and the values calculated using Eq. (12) (lines) when the reaction time of propionic acid is 15 ms or longer.

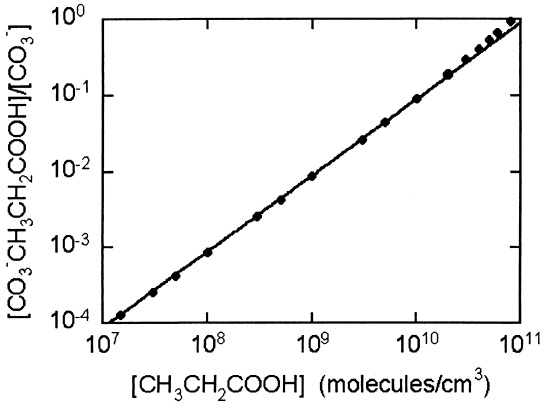

Fig. 9. Modelled quantity $[CO_3^-RCOOH]/[CO_3^-]$ plotted vs. the concentration of propionic acid with propionic acid reaction time of 15 ms. Good agreement is observed between the modelled values using the complete reaction system (dots) and the calculated values using Eq. (12) (lines) at atmospheric conditions.

7. Summary and conclusions

Ion molecule reactions of gaseous propionic, butyric, glyoxylic, pyruvic, and pinonic acids with several negative ion species have been investigated using a flow reactor. The latter was operated at a temperature of 293 ± 3 K and total gas pressures of 1.5, 9 hPa, and 40 hPa. Reactant and product ions were measured by a linear quadrupole and an ion trap mass spectrometer. The reactions proceeded either via proton transfer, ligand switching (for hydrated reactant ions), or clustering. A new proton transfer channel leading to alkylperoxy carboxylate radicals ($R_{-H}(OO\cdot)COO^-$) was observed for propionic, butyric, and pinonic acids. Reactions of glyoxylic acid with $CO_3^-(H_2O)_n$ proceeded only via proton transfer. Measured reaction rate coefficients for ligand switching of propionic and butyric acid all were close to the expected collision rate coefficients ($1.8–2.0 \times 10^9$ cm^3 molecule^{-1} s^{-1}). Our present experiments provide a basis for the quantitative detection of atmospheric gaseous propionic and butyric acids by IMRMS.

References

[1] T. Novakov, J.E. Penner, Nature 365 (1993) 823.
[2] O. Klemm, R.W. Talbot, D.R. Fitzgerald, K.I. Klemm, B.L. Lefer, J. Geophys. Res. 99 (1994) 1687.
[3] R.W. Talbot, B.W. Mosher, B.G. Heikes, D.J. Jacob, J.W. Munger, B.C. Daube, W.C. Keene, J.R. Maben, R.S. Artz, J. Geophys. Res. 100 (1995) 9335.
[4] K. Kawamura, L.-L. Ng, I.R. Kaplan, Environ. Sci. Technol. 19 (1985) 1082.
[5] H. Satsumabayashi, H. Kurita, Atmos. Environ. 24A (1990) 1443.
[6] S. Madronich, R.B. Chatfield, J.G. Calvert, G.K. Moortgat, B. Veyret, R. Lesclaux, Geophys. Res. Lett. 17 (1990) 2361.
[7] K. Kawamura, H. Kasukabe, O. Yasui, L.A. Barrie, Geophys. Res. Lett. 22 (1995) 1253.

[8] M.O. Andreae, R.W. Talbot, S.-M. Li, J. Geophys. Res. 92 (1987) 6635.
[9] F. Fehsenfeld, J. Calvert, R. Fall, P. Goldan, A.B. Guenther, C.N. Hewitt, B. Lamb, S. Liu, M. Trainer, H. Westberg, P. Zimmerman, Global Biogeochem. Cycles 6 (1992) 389.
[10] S. Hatakeyama, K. Izumi, T. Fukuyama, H. Akimoto, J. Geophys. Res. 94 (1989) 13 013.
[11] T. Hoffmann, R. Bandur, U. Marggraf, M. Linscheid, J. Geophys. Res. 103 (1998) 25 569.
[12] J.Z. Yu, R.C. Flagan, J.H. Seinfeld, Environ. Sci. Technol. 32 (1998) 2357.
[13] S. Madronich, J.G. Calvert, J. Geophys. Res. 95 (1990) 5697.
[14] P.D. Lightfoot, R.A. Cox, J.N. Crowley, M. Destriau, G.D. Hayman, M.E. Jenkin, G.K. Moortgat, F. Zabel, Atmos. Environ. 26A (1992) 1805.
[15] K. Kawamura, L.-L. Ng, I.R. Kaplan, Environ. Sci. Technol. 19 (1985) 1082.
[16] D. Grosjean, Environ. Sci. Technol. 1989 (23) 1506.
[17] Y. Suzuki, Analytica Chimica Acta 353 (1997) 227.
[18] U. Hofmann, D. Weller, Ch. Ammann, E. Jork, J. Kesselmeier, Atmos. Environ. 31 (1997) 1275.
[19] I.G. Kavouras, N. Mihalopoulos, E.G. Stephanou, Geophys. Res. Lett. 26 (1999) 55.
[20] Y.-N. Lee, X. Zhou, K. Hallock, J. Geophys. Res. 100 (1995) 25 933.
[21] Y. Yokouchi, Y. Ambe, Atmos. Environ. 19 (1985) 1271.
[22] T. Hoffmann, J.R. Odum, F. Bowman, D. Collins, D. Klockow, R.C. Flagan, J.H. Seinfeld, J. Atmos. Chem. 26 (1997) 189.
[23] T.S. Christoffersen, J. Hjorth, O. Horie, N.R. Jensen, D. Kotzias, L.L. Molander, P. Neeb, L. Ruppert, R. Winterhalter, A. Virkkula, K. Wirtz, B.R. Larsen, Atmos. Environ. 32 (1998) 1657.
[24] I.G. Kavouras, N. Mihalopoulos, E.G. Stephanou, Nature 395 (1998) 683.
[25] J. Viidanoja, Th. Reiner, F. Arnold, Int. J. Mass Spectrom. 181 (1998) 31.
[26] O. Möhler, F. Arnold, J. Atmos. Chem. 13 (1991) 33.
[27] O. Möhler, T. Reiner, F. Arnold, J. Chem. Phys. 97 (1992) 8233.
[28] M.D. Taylor, J. Bruton, J. Am. Chem. Soc. 74 (1952) 4151.
[29] D.K. Bohme, G.I. Mackay, S.D. Tanner, J. Am. Chem. Soc. 101 (1979) 3724.
[30] P.H. Wine, R.J. Astalos, R.L. Mauldin III, J. Phys. Chem. 89 (1985) 2620.
[31] W. Paul, H.P. Reinhard, U. von Zahn, Z. Phys. 152 (1958) 143.
[32] S.G. Lias, J.E. Bartmess, J.F. Liebmann, J.L. Holmes, R.D. Levin, W.G. Mallard, J. Phys. Chem. Ref. Data 17 (1988) (suppl. 1).
[33] T. Su, W.J. Chesnavich, J. Phys. Chem. 76 (1982) 5183.
[34] F. Eisele, D. Tanner, J. Geophys. Res. 98 (1993) 9001.
[35] H. Fischer, A.E. Waibel, M. Welling, F.G. Wienhold, T. Zenker, P.J. Crutzen, F. Arnold, V. Bürger, J. Schneider, A. Bregman, J. Lelieveld, P.C. Siegmund, J. Geophys. Res. 102 (1997) 23 559.
[36] O. Möhler, F. Arnold, Geophys. Res. Lett. 19 (1992) 1763.
[37] J. Schneider, V. Bürger, F. Arnold, J. Geophys. Res. 102 (1997) 25 501.
[38] F. Arnold, V. Bürger, B. Droste-Franke, F. Grimm, A. Krieger, J. Schneider, T. Stilp, Geophys. Res. Lett. 24 (1997) 3017.
[39] Th. Reiner, O. Möhler, F. Arnold, J. Geophys. Res. 103 (1998) 31 309.
[40] F. Arnold, G. Hauck, Nature 315 (1985) 307.
[41] O. Möhler, T. Reiner, F. Arnold, Rev. Sci. Instrum. 64 (1993) 1199.
[42] L.G. Huey, E.R. Lovejoy, Int. J. Mass Spectrom. Ion Processes 155 (1996) 133.